



Advancements Toward Oil-Free Rotorcraft Propulsion

*Samuel A. Howard and Robert J. Bruckner
Glenn Research Center, Cleveland, Ohio*

*Kevin C. Radil
U.S. Army Research Laboratory, Glenn Research Center, Cleveland, Ohio*

NASA STI Program . . . in Profile

Since its founding, NASA has been dedicated to the advancement of aeronautics and space science. The NASA Scientific and Technical Information (STI) program plays a key part in helping NASA maintain this important role.

The NASA STI Program operates under the auspices of the Agency Chief Information Officer. It collects, organizes, provides for archiving, and disseminates NASA's STI. The NASA STI program provides access to the NASA Aeronautics and Space Database and its public interface, the NASA Technical Reports Server, thus providing one of the largest collections of aeronautical and space science STI in the world. Results are published in both non-NASA channels and by NASA in the NASA STI Report Series, which includes the following report types:

- **TECHNICAL PUBLICATION.** Reports of completed research or a major significant phase of research that present the results of NASA programs and include extensive data or theoretical analysis. Includes compilations of significant scientific and technical data and information deemed to be of continuing reference value. NASA counterpart of peer-reviewed formal professional papers but has less stringent limitations on manuscript length and extent of graphic presentations.
- **TECHNICAL MEMORANDUM.** Scientific and technical findings that are preliminary or of specialized interest, e.g., quick release reports, working papers, and bibliographies that contain minimal annotation. Does not contain extensive analysis.
- **CONTRACTOR REPORT.** Scientific and technical findings by NASA-sponsored contractors and grantees.

- **CONFERENCE PUBLICATION.** Collected papers from scientific and technical conferences, symposia, seminars, or other meetings sponsored or cosponsored by NASA.
- **SPECIAL PUBLICATION.** Scientific, technical, or historical information from NASA programs, projects, and missions, often concerned with subjects having substantial public interest.
- **TECHNICAL TRANSLATION.** English-language translations of foreign scientific and technical material pertinent to NASA's mission.

Specialized services also include creating custom thesauri, building customized databases, organizing and publishing research results.

For more information about the NASA STI program, see the following:

- Access the NASA STI program home page at <http://www.sti.nasa.gov>
- E-mail your question via the Internet to help@sti.nasa.gov
- Fax your question to the NASA STI Help Desk at 443-757-5803
- Telephone the NASA STI Help Desk at 443-757-5802
- Write to:
NASA Center for AeroSpace Information (CASI)
7115 Standard Drive
Hanover, MD 21076-1320



Advancements Toward Oil-Free Rotorcraft Propulsion

*Samuel A. Howard and Robert J. Bruckner
Glenn Research Center, Cleveland, Ohio*

*Kevin C. Radil
U.S. Army Research Laboratory, Glenn Research Center, Cleveland, Ohio*

Prepared for the
65th Annual Forum and Technology Display (AHS Forum 65)
sponsored by the American Helicopter Society
Grapevine, Texas, May 27–29, 2009

National Aeronautics and
Space Administration

Glenn Research Center
Cleveland, Ohio 44135

Acknowledgments

The authors would like to acknowledge the fiscal support of NASA's Subsonic Rotary Wing Program, part of the Aeronautics Research Mission Directorate.

This report contains preliminary findings,
subject to revision as analysis proceeds.

Trade names and trademarks are used in this report for identification only. Their usage does not constitute an official endorsement, either expressed or implied, by the National Aeronautics and Space Administration.

Level of Review: This material has been technically reviewed by technical management.

Available from

NASA Center for Aerospace Information
7115 Standard Drive
Hanover, MD 21076-1320

National Technical Information Service
5285 Port Royal Road
Springfield, VA 22161

Available electronically at <http://gltrs.grc.nasa.gov>

Advancements Toward Oil-Free Rotorcraft Propulsion

Samuel A. Howard and Robert J. Bruckner
National Aeronautics and Space Administration
Glenn Research Center
Cleveland, Ohio 44135

Kevin C. Radil
U.S. Army Research Laboratory
Glenn Research Center
Cleveland, Ohio 44135

Abstract

NASA and the Army have been working for over a decade to advance the state-of-the-art (SOA) in Oil-Free Turbomachinery with an eye toward reduced emissions and maintenance, and increased performance and efficiency among other benefits. Oil-Free Turbomachinery is enabled by oil-free gas foil bearing technology and relatively new high-temperature tribological coatings. Rotorcraft propulsion is a likely candidate to apply oil-free bearing technology because the engine size class matches current SOA for foil bearings and because foil bearings offer the opportunity for higher speeds and temperatures and lower weight, all critical issues for rotorcraft engines. This paper describes an effort to demonstrate gas foil journal bearing use in the hot section of a full-scale helicopter engine core. A production engine hot-core location is selected as the candidate foil bearing application. Rotordynamic feasibility, bearing sizing, and load capability are assessed. The results of the program will help guide future analysis and design in this area by documenting the steps required and the process utilized for successful application of oil-free technology to a full-scale engine.

Introduction

Previously, NASA conducted a feasibility study to assess the potential for an Oil-Free rotorcraft core (Ref. 1). The analysis, based upon a rotordynamic study of a T700 engine core, concluded that gas foil bearing technology was advanced to the point that an Oil-Free core was technologically possible. A General Electric T700 engine was used as the model because it is common in the rotorcraft community, and it is a reasonable size class for the current SOA of foil bearings. Following from this analysis, an experimental effort has begun to demonstrate a gas foil bearing at the hot-end of a T700 core rotor. NASA and the Army have acquired used engine flight hardware from a T700, seen in Figure 1, to conduct the demonstration. Using a phased approach, the engine core will eventually be rotated on gas foil bearings to demonstrate successful full-scale Oil-Free engine operation.

NASA, in conjunction with industry, has developed a four-step process for integration of gas foil bearings into turbomachinery (Ref. 2). The four steps are: 1) assess the

rotordynamic feasibility of the application, 2) component testing of candidate bearing designs, 3) rotordynamic system testing with a simulated rotor and the selected bearing design from step 2, and 4) full-scale demonstration after successful rotordynamic simulation. In this paper, the first two steps are described for the T700 hot-section application. A more relevant rotordynamic feasibility study is done, and a foil journal bearing is tested for load capacity and power loss. The bearing size and design are based upon the conclusions of the feasibility study, and analytical bearing design tools. The results indicate that a T700 core rotor is a viable candidate for a hot-section gas foil bearing, and a 76.2- by 63.5-mm bearing is chosen as the initial size for simulation testing.

A follow-on activity, based upon successful completion of this work, will focus on spinning the core rotor with the foil journal bearing tested here installed in the hot-end of the rotor (the location between the compressor and the turbine, hereafter called the rear bearing). That work will represent step 3 of the four-step process. This combined effort compliments work being done by the engine manufacturer.

Bearing and Rotor Design Considerations

In general, Oil-Free Turbomachinery rotors are designed to be rigid with respect to the operating speed range. Shafting is often large in diameter and thin-walled in order to keep the weight low and the stiffness high. Increased rotor diameter also results in larger load capacities for foil bearings. This is in direct opposition to typical rolling element bearing shaft designs where rotor diameters at bearing locations are often kept small to reduce the bearing DN (diameter times speed) rating for longer useful life. Thus, in retrofitting a rotor bearing system designed for rolling element bearings, one must address this contradiction.

The T700 rotor of interest (compressor rotor) in this effort is not extremely small in diameter because it is hollow with the power turbine rotor running inside. However, it is still fairly flexible, and in fact, has a bending critical speed below the idle speed. Ideally, if this system were a complete redesign, an attempt would be made to stiffen the rotor to move the bending critical speed above the maximum operating speed. However, the size and layout of the rotor system is constrained to fit inside the existing engine envelope

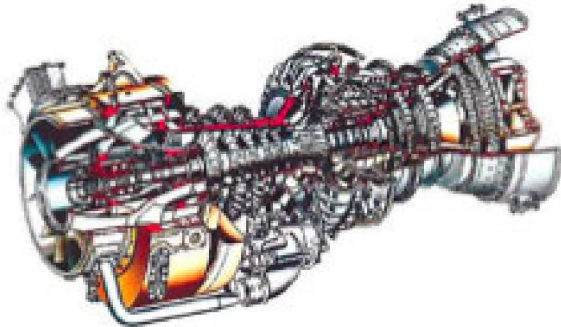


Figure 1.—Cut-away view of GE T700 engine.

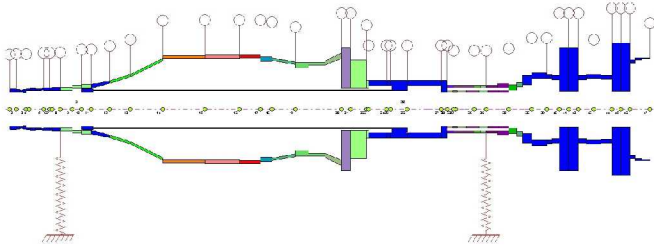


Figure 2.—Rotordynamic model of GE T700 core rotor with ball bearing in front, foil bearing in rear.

precluding a major redesign. Thus, successful Oil-Free conversion of the hot-end of the T700 rotor depends upon the ability to accelerate the rotor through the bending critical speed. In order to traverse a critical speed, particularly a critical speed with a bending mode shape, there must be adequate system damping to limit the amplitude of vibration at the critical locations of the rotor, such as the compressor and turbine blade tips. Therefore, in this case, there must be enough damping in the front rolling element bearing and the rear foil bearing to sufficiently suppress the vibration levels at the critical speed.

In the previous feasibility study (Ref. 1), it was determined that foil bearings in both the front and rear bearing locations of the core rotor would likely offer sufficient damping to successfully navigate the original T700 operating envelope. Two rotor designs were considered, one slightly modified from the original geometry to accept foil bearings, but not change the structural characteristics, and one modified to accept foil bearings while stiffening the rotor to force the bending critical speed above the maximum operating speed. The stiffer rotor design results in a more robust design by moving the bending critical speed above the maximum operating speed. Also, by increasing the bearing span, the rotor weight is better distributed, allowing a more heavily loaded front bearing which results in increased system stability. Unfortunately, the previous study was conducted under the auspices of having the freedom to change the rotor layout and use foil bearings in both the front and rear locations. Therefore, it has little applicability to this effort in which the front rolling element bearing is retained and the geometry of the rotor is constrained to fit in the existing architecture. In other words, the previous analysis assumed a complete redesign of the engine, where the current effort is a

less drastic retrofit. Therefore, another rotordynamic analysis was conducted with the specific bearing configuration planned for the T700 retrofit to determine the feasibility of success.

Rotordynamics

The previous feasibility analysis indicated that a 76.2-mm diameter by 50.8-mm length foil bearing would yield desirable rotordynamic performance. That analysis was aimed at determining the feasibility of a foil bearing supported engine rotor, and sought to find a bearing size with potential for success. The analysis does not suggest that the bearing size found is the only possible size. Therefore, in choosing a bearing size to analyze and test in this work, a bearing with a 76.2-mm diameter and 63.4-mm length is used because that size had been manufactured before, and therefore was faster and less costly to produce. The added length increases the load carrying capability of the bearing, while potentially decreasing the stability due to a lighter unit loading. As long as the rotordynamics of the system with the larger bearing are acceptable, the added length is viewed as a benefit in the context of added load capacity.

The rotor model used previously is resurrected and used for the current rotordynamic analysis. Figure 2 shows the model with the bearing locations indicated by zig-zag lines and the added mass for blades and other non-structural components represented by circles.

A baseline model was run in the original analysis to verify that the model accurately represents the actual engine. To that end, the first three critical speeds of the rotor were calculated and compared to the actual critical speeds of the engine as measured by the manufacturer. Table 1 lists the calculated critical speeds and the error with respect to the measured critical speeds as reported in (Ref. 1). Since the errors are quite small, the model is assumed to represent the engine well. For the current effort, as stated earlier, there is little freedom to modify the rotor significantly in the area where the foil bearing will be located. Therefore, the foil bearing is modeled in the same axial location, and it is assumed the geometry of the rotor will not be changed enough to significantly alter the structural characteristics of the rotor. The bearing properties are changed to reflect those of the chosen foil bearing size. Table 2 list the pertinent bearing parameters used in the model. The bearing force coefficients are calculated using the most recent version of the bearing analysis tool used in the previous feasibility analysis (Refs. 3 and 4).

TABLE 1.—CRITICAL SPEED AND MASS COMPARISONS OF BASELINE MODEL TO EMPIRICAL ENGINE DATA

Characteristic	Baseline model predictions	Error compared to engine
1 st critical speed	6,260 rpm	0.6 %
2 nd critical speed	12,700 rpm	3.5 %
3 rd critical speed	26,600 rpm	1.2 %
4 th critical speed	76,600 rpm	not measured
Mass	21.9 kg	-1.7 %

TABLE 2.—BEARING DYNAMIC FORCE COEFFICIENTS
USED IN ROTORDYNAMIC MODEL FOR
76.2 mm BY 63.5 mm BEARING

Speed, rpm	Kxx(N/m) Cxx(Ns/m)	Kxy Cxy	Kyx Cyx	Kyy Cyy
10,000	1.42e7 3.89e3	9.75e5 -2.30e3	1.55e6 1.75e3	1.07e7 4.38e3
30,000	1.39e7 1.30e3	-4.16e5 -4.10e2	1.71e6 6.22e2	1.36e7 1.22e3
50,000	1.48e7 7.44e2	-3.14e5 -1.46e2	2.02e6 2.37e2	1.42e7 5.60e2

Since the current analysis is based upon spinning the rotor with a foil bearing at the rear, and a ball bearing at the front, the front bearing (outboard of the compressor) remains the same as in the baseline rotor configuration. Therefore, the rotordynamic coefficients used in the baseline analysis are used again here. The configuration analyzed and proposed here is the most likely to be implemented first in a production engine for at least two reasons. First, a majority of the benefits of oil-free bearing technology can be realized by eliminating the oil-lubricated bearing from the hot-section. Second, utilizing a ball bearing in the front section eliminates the need for an oil-free thrust bearing, the technology of which is not as advanced as oil-free journal bearings. Thus, the configuration offers a way to relatively quickly reap many of the oil-free benefits, with less development effort and risk. It is a configuration being considered by several engine manufacturers in various applications.

The results of the rotordynamic analysis indicate that the combined ball bearing/foil bearing configuration is feasible. The critical speeds and mode shapes of the resulting system are only slightly changed from the original engine. Table 3 lists the critical speeds of the baseline model compared to the current model. One can see that the foil bearing at the rear has very little effect on the natural frequencies of the rotor system. The foil bearing has similar stiffness properties to the rolling element bearing of the baseline configuration resulting in the small changes in critical speeds. However, the stability of the system is just as important as the frequencies of the critical speeds.

TABLE 3.—CRITICAL SPEED COMPARISONS OF BASELINE
MODEL TO CURRENT MODEL WITH REAR FOIL BEARING

Characteristic	Baseline model predictions	Current model predictions
1 st critical speed	6,260 rpm	7,300 rpm
2 nd critical speed	12,700 rpm	12,900 rpm
3 rd critical speed	26,600 rpm	27,200 rpm
4 th critical speed	76,600 rpm	77,000 rpm

A stability analysis indicates that all three modes below the maximum speed of the rotor are stable up to and including 50,000 rpm which represents a roughly 10% over-speed condition. Figure 3 is a plot of the log decrement of the lowest three forward mode shapes as a function of speed. The system

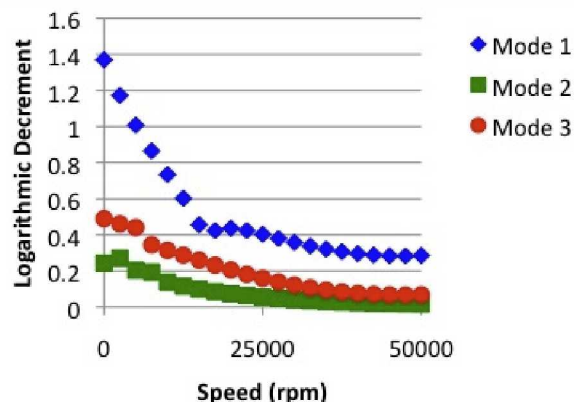


Figure 3.—Logarithmic decrement versus speed for the first three mode shapes.

is considered stable as long as the log decrement is positive. Based upon the critical speed analysis and the stability analysis, a 76.2-mm diameter by 63.5-mm long foil bearing appears to be a possible bearing size for the rear of the T700 core rotor.

Preliminary Bearing Tests

Given the promising results of the rotordynamic analysis, a 76.2- by 63.5-mm foil bearing was chosen for preliminary testing. The following tests can be thought of as preliminary screening to determine if the bearing size is appropriate for the T700 application. The bearing is of the generation III type as defined in DellaCorte and Valco (Ref. 5). A short description of a generation III foil bearing is one in which the compliant support structure is designed with variable stiffness in at least two directions (i.e., axial and radial, axial and circumferential, etc.). By comparison, generation I and II bearings have structural properties that are constant everywhere and vary in only one direction, respectively. In general, bearing performance improves from generation I to II and from II to III, such that generation III bearings are considered to be the SOA in foil bearing technology.

The foil bearing tested was of the design described in Heshmat (Ref. 6). Typical bearing qualification tests include load capacity, and torque vs. speed vs. load (torque data is used to generate a power loss map described in (Ref. 7)). Unfortunately, with the bearing size of interest here, a load capacity test was not possible because the maximum load that can be applied by the test rig is approximately 222 N. The anticipated load capacity of the 76.2- by 63.5-mm bearing, using a previously developed empirical rule-of-thumb (Ref. 5), is around 1,800 N at 18,000 rpm (the test speed). However, the static load (weight of the rotor) the bearing will be required to support in the T700 application, 170 N, is within the capabilities of the test rig. Similarly, a complete power loss map was not possible due to limited speed and load capabilities of the existing test rig relative to a bearing of this size.

The test rig, shown in Figure 4, was designed to do start/stop life testing of smaller bearings. As such, it has a maximum speed of 21,000 rpm and maximum load of 222 N. Therefore, only preliminary bearing testing is conducted to determine how well the bearing performs subjected to the steady state rotor weights of 170 and 145 N as described below.

The test rig allows for two different methods of loading a test bearing. In the first method, a pneumatic actuator is used to pull downward on the test bearing by way of a cable and yoke mechanism. Unfortunately, for the large loads of interest here, the cable mechanism also constrains the bearing in the rotational direction, making it impossible to accurately measure torque in this configuration. In the second method of applying load to the bearing, concentric rings of a very dense material (Anvaloy) are mounted on the outside diameter of the bearing, as seen in Figure 5. The rings are balanced in an attempt to minimize any rotational force due to non-concentricity that would affect the torque measurement. The advantage of the first loading method is the ability to load the bearing between zero and the upper limits of the test rig, approximately 222 N. The obvious disadvantage is the lack of capability to measure torque. The second method allows for measurement of torque, but limits the applied load capability to several discrete loads up to a maximum of 145 N. From here forward, the concentric ring loading mechanism is referred to as a dead-weight loading since the load is passive.

In order to test the capability of the bearing to support a steady-state load of 170 N, the cable loading mechanism was used. To gauge the power loss, though, a second test was conducted using the dead-weight loads. Typically, a power loss map is generated to determine if a bearing is operating in a light, moderate, or heavy loading regime, as described in (Ref. 7). However, since this was a preliminary screening test, no attempt was made to generate a full power loss map, rather the power loss with the maximum possible dead load, 145 N, was measured. The value of this test was simply to determine if the power loss at a load near that of the expected load is consistent with a healthy load condition. If the power loss were excessive, it would suggest the bearing size may not be appropriate for the application.

Before any testing was conducted, the bearing was broken-in, or conditioned, by completing 5,800 start-up and shut-down cycles at 538 °C. This conditioning routine is typical to obtain a conforming surface between the journal and the bearing, and to improve the surface finish for better performance (Ref. 8). A photograph of the conditioned bearing shows normal regions of wear from the break-in process in Figure 6.

The bearing had three thermocouples (the leads can also be seen in Fig. 6) installed at the fixed end of the top foil. The thermocouples were attached to the spacer block in the gap between the fixed and free ends of the foil as shown in Figure 7. They were located outboard, in the middle, and inboard of the bearing in the axial direction relative to the motor side of the journal. The thermocouple data was used in

conjunction with the torque data to monitor the health of the bearing, and to compare to typical foil bearing behavior for screening purposes during the test with the dead-weight load.



Figure 4.—Photograph of the test rig used for GE T700 bearing tests.



Figure 5.—Photograph of the test bearing with concentric dead weight loading rings and torque arm.

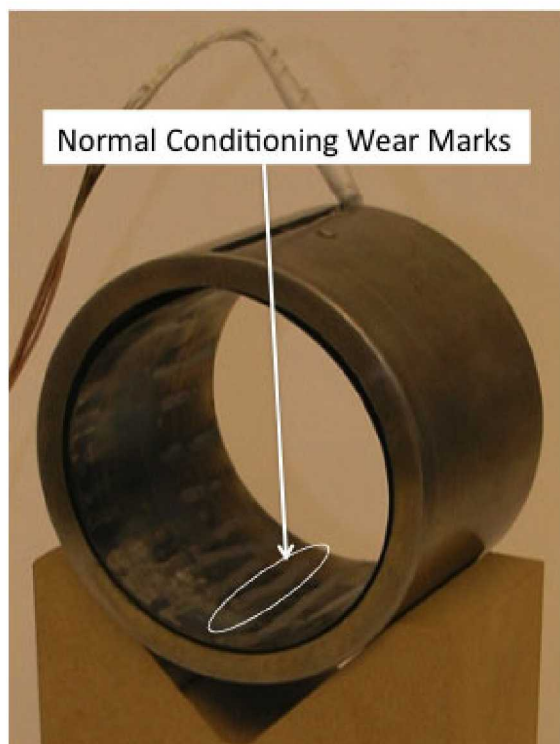


Figure 6.—Photograph of the test bearing after conditioning showing normal wear.

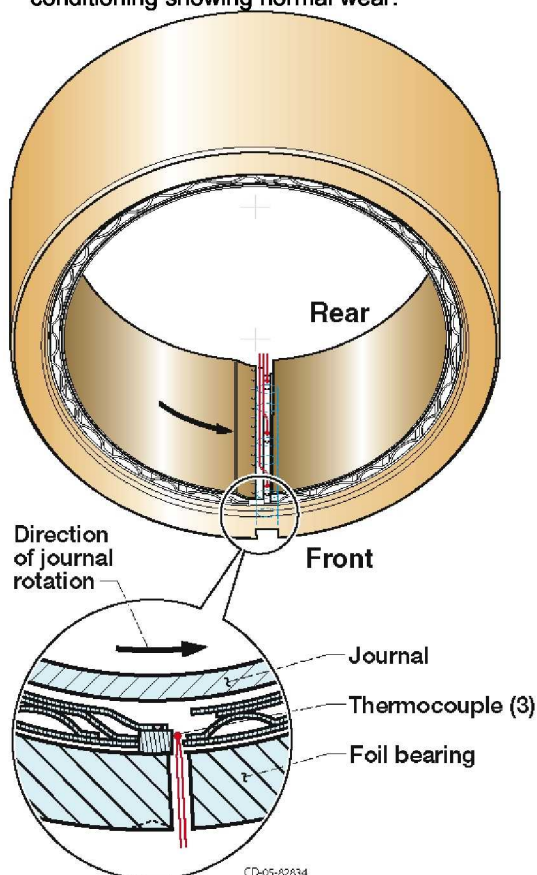


Figure 7.—Schematic showing the thermocouple location inside the test bearing.

Preliminary Bearing Test Results

As described above, the first test was to apply a 170 N load via a cable and pneumatic loader. With 170 N, the bearing ran for about an hour with no problems observed. The purpose of this test was to see if the bearing would lift-off under an applied load consistent with the T700 application. The determination of lift-off is based mostly on experience, but the bearing was clearly floating and was free to drift back and forth on the journal. This first test served to verify that the bearing size was likely sufficient.

Next, the concentric load rings were installed on the bearing, and the more quantitative, yet still preliminary, dead-weight test was conducted. Figure 5 shows the bearing with the three concentric dead-weight loads mounted. One can also see the torque arm that attaches by cable to a load cell for measuring the running torque. During the dead weight test, three objectives were met. First, the temperature was measured from start-up until a steady state thermal condition was reached. Second, running torque with a 145 N dead-weight load (as close to 170 N as possible using existing dead-weights) was measured for a power loss assessment. Lastly, speed versus time data for a coast-down event was recorded to observe the speed at which the bearing started to rub (touch-down or lift-off speed).

Figure 8 shows the temperature recorded by the three thermocouples as the bearing reached steady-state at about 45 min. into the test. Two observations are immediately obvious from the figure: the steady state-operating temperature at 18,000 rpm is around 60 to 70 °C depending on axial location. Interestingly, the outboard temperature was very similar to the middle temperature, while the inboard temperature was about 10 °C lower during most of the test. This was most likely due to the positioning of the thermocouples, wherein the outboard thermocouple was located about 6 mm in from the edge of the foil, while the inboard was located very near the edge of the foil. The reason for the discrepancy was simply a matter of installation logistics. The thermocouples enter the gap from the outer diameter through holes, and then are bent to align with the spacer block. In this case, the technician bent all the thermocouples the same direction such that the outboard thermocouple was bent toward the middle of the bearing upon exiting the hole, and the inboard thermocouple was bent away from the middle as it exited the hole. This cause may not be the sole cause, as there could be other contributing factors. One such factor is the relative looseness of the inboard and outboard edges. If the bearing were tighter, due to manufacturing variation, on the outboard edge, the above observation could result. The variation in temperature is not a reason for concern, and the main conclusion one can make from this data is that the bearing performed well, based upon temperature, for a load of 145 N at 18,000 rpm. Temperatures of 60 to 70 °C are relatively low for an uncooled bearing (Ref. 9), indicating that 145 N is likely a light-load condition for the bearing at this speed.

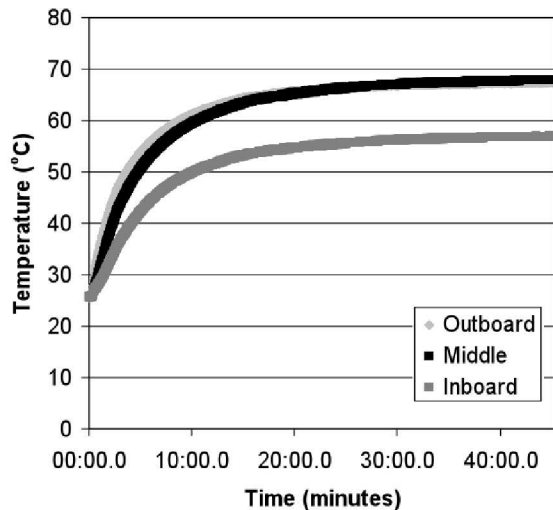


Figure 8.—Plot of temperature at the fixed end of the foil.

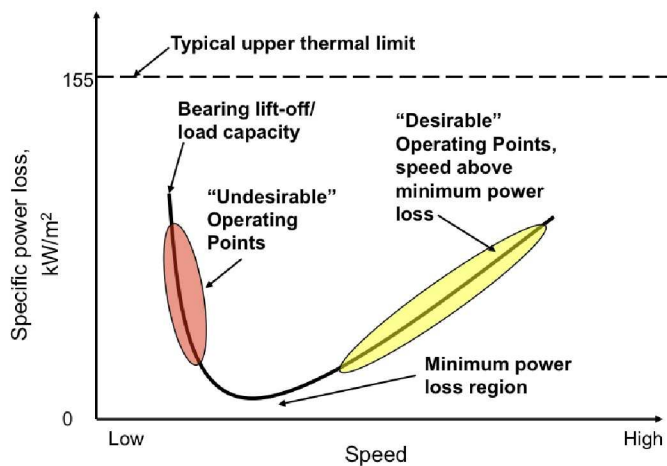


Figure 9.—Typical power loss gas foil bearing performance map.

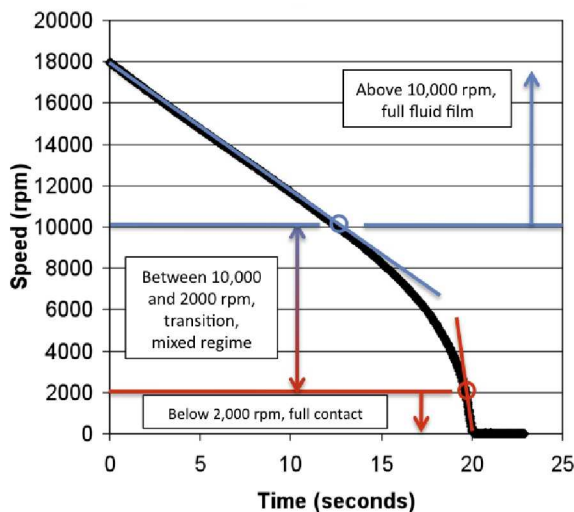


Figure 10.—Coast-down speed plot.

It has been observed that one can use power loss as a measure of performance in gas foil journal bearings (Ref. 7). Power loss is calculated from the torque measurement, and represents an indication of how much heat is generated in the bearing. There is a significant speed effect and to a lesser extent a load effect on power loss. At very low speed, the power loss is high due either to extreme shear rates of the gas film or rubbing if the speed is below the lift-off speed. As speed increases, power loss drops to a minimum, then begins to rise again. Figure 9 shows a sample power loss map (not for this bearing). For various reasons, the desirable operating regime is at speed and load combinations that keep the bearing on the high side (with respect to speed) of the minimum power loss. A full power loss map was not created in this work because of the limited test rig capabilities. However, a torque measurement of 0.094 N-m at 18,000 rpm and a dead-weight load of 145 N was measured when the temperature reached steady-state during the test. Torque of 0.094 N-m corresponds to a power loss of 37 kW/m², a relatively low number based upon experimental results where typical power loss levels at failure are approximately 155 kW/m². While a full power loss map would need to be constructed to fully characterize the bearing, this one data point suggests that at 18,000 rpm under a load of 145 N, the bearing tested is near the minimum power loss level. An increase in speed, up to the T700 full speed of roughly 45,000 rpm, would likely put the power loss in the desired zone above the minimum power loss level.

The final screening test to characterize the bearing was a coast-down test. The bearing was run at 18,000 rpm and allowed to warm-up to a steady-state temperature condition as in the first test. The motor power was shut-off, and the speed was recorded as the rotor coasted to a stop. Plotting speed versus time, as in Figure 10, one can see the approximate speed at which the bearing begins to contact the rotor, i.e., the touch-down, or lift-off speed (called the lift-off speed from here on). Looking at Figure 10, the speed of the rotor decreases with positive curvature from 18,000 rpm to approximately 8,000 rpm (the curvature of the speed curve is the third derivative of position with respect to time, called jerk). After 8,000 rpm, the sign of jerk changes from positive to negative, and the speed trace curves downward. It is believed the transition from positive to negative jerk marks the transition from a fully hydrodynamic fluid film to a boundary type lubrication regime. That transition also translates roughly to the speed on the performance map where the power loss minimum occurs. In this case, that speed is approximately 10,000 rpm, as seen in Figure 9. At some speed, the fluid film completely breaks down, and the slope of the curve becomes nearly vertical, indicating full sliding contact, which can be seen around 2,000 rpm on the coast-down plot. Typically, the minimum power loss is 2 to 6 times the lift-off speed (Refs. 7 and 10), which is consistent with the coast-down plot here where lift-off speed is near 2,000, and 10,000 rpm is near the transition to a full film.

All three of the test results point to the same conclusion, that a 145 to 170 N load on a 76.2- by 63.4-mm foil journal

bearing is a reasonable load at 18,000 rpm. The T700 application has a speed range requirement of about 20,000 to 45,000 rpm. Though the three screening tests were limited in scope, due to test rig constraints, they all indicate that the bearing size is viable for further consideration in the application.

Conclusions

The first two steps of a four-step design process have been completed for assessing the performance of a gas foil journal bearing in the hot-section of a rotorcraft propulsion system. The rotordynamic feasibility study concluded that a bearing with a 76.2-mm diameter and 63.5-mm length would be a proper size for the applied load of 170 N, and would offer sufficient rotordynamic performance based upon predicted bearing force coefficients.

The series of tests performed here indicate: 1) The bearing could lift off with a 170 N load and maintain operation for a prolonged period of time, 2) The bearing running with a 145 N dead-weight load reached steady state operating temperatures of 60 to 70 °C, which were relatively low, indicating that the bearing was not heavily stressed, 3) The power loss of 37 kW/m² at 18,000 rpm with a 145 N load was low compared to typical values observed at failure of 155 kW/m², and 4) The lift-off speed was found to be around 2,000 rpm and the transition to full film occurs at roughly 5 times that speed at 10,000 rpm, thus, the T700 speed range of 20,000 to 45,000 rpm will be slightly above where the transition to a full film occurs.

In summary, all indications are that the tested bearing is expected to perform well in the hot-section of a T700 rotorcraft propulsion engine. With a viable bearing design, the future plan is to move ahead with the third step of the design process, rotordynamic simulator testing.

References

1. Howard, S.A., Bruckner, R.J., DellaCorte, C., and Radil, K.C., "Preliminary Analysis for an Optimized Oil-Free Rotorcraft Engine Concept," NASA/TM—2008-215064, 2008.
2. Valco, M.J., and DellaCorte, C., "Emerging Oil-Free Turbomachinery for Military Propulsion and Power Applications," Proceedings of the Army Sciences Conference, Ft. Lauderdale, FL, 2003.
3. Carpino, M., and Talmadge, G., "A Fully Coupled Finite Element Formulation for Elastically Supported Foil Journal Bearings," *Tribology Transactions*, Vol. 46, pp. 560–565, 2003.
4. Carpino, M., and Talmadge, G., "Prediction of Rotordynamic Coefficients in Gas Lubricated Foil Journal Bearings with Corrugated Sub-Foils," *Tribology Transactions*, Vol. 49, pp. 400–409, 2006.
5. DellaCorte, C., and Valco, M.J., "Load Capacity Estimation of Foil Air Journal Bearings for Oil-Free Turbomachinery Applications," *Tribology Transactions*, Vol.43, No. 4, pp.795–801, 2000.
6. Heshmat, H., "High Load Capacity Compliant Foil Hydrodynamic Journal Bearing," U.S. Patent No. 5,988,885, Nov. 1999.
7. DellaCorte, C., Radil, K.J., Bruckner, R.J., and Howard, S.A., "A Preliminary Foil Gas Bearing Performance Map," NASA/TM—2006-214343, 2006.
8. Radil, K.J., and DellaCorte, C., "The Effect of Journal Roughness and Foil Coatings on the Performance of Heavily Loaded Foil Air Bearings," NASA/TM—2001-210941, 2001.
9. Radil, K.J., DellaCorte, C., and Zeszotek, M., "Thermal Management Techniques for Oil-Free Turbomachinery Systems," NASA/TM—2006-214358, 2006.
10. DellaCorte, C., Radil, K.J., Bruckner, R.J., and Howard, S.A., "Design, Fabrication and Performance of Open Source Generation I and II Compliant Hydrodynamic Gas Foil Bearings," NASA/TM—2007-214691, 2007.

REPORT DOCUMENTATION PAGE				Form Approved OMB No. 0704-0188	
<p>The public reporting burden for this collection of information is estimated to average 1 hour per response, including the time for reviewing instructions, searching existing data sources, gathering and maintaining the data needed, and completing and reviewing the collection of information. Send comments regarding this burden estimate or any other aspect of this collection of information, including suggestions for reducing this burden, to Department of Defense, Washington Headquarters Services, Directorate for Information Operations and Reports (0704-0188), 1215 Jefferson Davis Highway, Suite 1204, Arlington, VA 22202-4302. Respondents should be aware that notwithstanding any other provision of law, no person shall be subject to any penalty for failing to comply with a collection of information if it does not display a currently valid OMB control number.</p> <p>PLEASE DO NOT RETURN YOUR FORM TO THE ABOVE ADDRESS.</p>					
1. REPORT DATE (DD-MM-YYYY) 01-03-2010		2. REPORT TYPE Technical Memorandum		3. DATES COVERED (From - To)	
4. TITLE AND SUBTITLE Advancements Toward Oil-Free Rotorcraft Propulsion				5a. CONTRACT NUMBER	
				5b. GRANT NUMBER	
				5c. PROGRAM ELEMENT NUMBER	
6. AUTHOR(S) Howard, Samuel, A.; Bruckner, Robert, J.; Radil, Kevin, C.				5d. PROJECT NUMBER	
				5e. TASK NUMBER	
				5f. WORK UNIT NUMBER WBS 877868.02.07.03.01.01.04	
7. PERFORMING ORGANIZATION NAME(S) AND ADDRESS(ES) National Aeronautics and Space Administration John H. Glenn Research Center at Lewis Field Cleveland, Ohio 44135-3191				8. PERFORMING ORGANIZATION REPORT NUMBER E-17147	
9. SPONSORING/MONITORING AGENCY NAME(S) AND ADDRESS(ES) National Aeronautics and Space Administration Washington, DC 20546-0001				10. SPONSORING/MONITOR'S ACRONYM(S) NASA	
				11. SPONSORING/MONITORING REPORT NUMBER NASA/TM-2010-216094	
12. DISTRIBUTION/AVAILABILITY STATEMENT Unclassified-Unlimited Subject Categories: 07 and 37 Available electronically at http://gltrs.grc.nasa.gov This publication is available from the NASA Center for AeroSpace Information, 443-757-5802					
13. SUPPLEMENTARY NOTES					
14. ABSTRACT <p>NASA and the Army have been working for over a decade to advance the state-of-the-art (SOA) in Oil-Free Turbomachinery with an eye toward reduced emissions and maintenance, and increased performance and efficiency among other benefits. Oil-Free Turbomachinery is enabled by oil-free gas foil bearing technology and relatively new high-temperature tribological coatings. Rotorcraft propulsion is a likely candidate to apply oil-free bearing technology because the engine size class matches current SOA for foil bearings and because foil bearings offer the opportunity for higher speeds and temperatures and lower weight, all critical issues for rotorcraft engines. This paper describes an effort to demonstrate gas foil journal bearing use in the hot section of a full-scale helicopter engine core. A production engine hot-core location is selected as the candidate foil bearing application. Rotordynamic feasibility, bearing sizing, and load capability are assessed. The results of the program will help guide future analysis and design in this area by documenting the steps required and the process utilized for successful application of oil-free technology to a full-scale engine.</p>					
15. SUBJECT TERMS Gas bearings; Foil bearings; Rotor dynamics					
16. SECURITY CLASSIFICATION OF:			17. LIMITATION OF ABSTRACT UU	18. NUMBER OF PAGES 13	19a. NAME OF RESPONSIBLE PERSON STI Help Desk (email: help@sti.nasa.gov)
a. REPORT U	b. ABSTRACT U	c. THIS PAGE U			19b. TELEPHONE NUMBER (include area code) 443-757-5802

